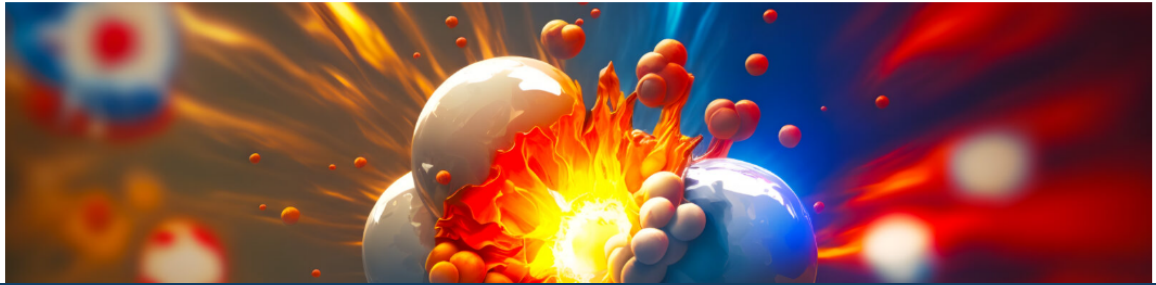
# THE PHYSICS AND CHEMISTRY OF THE HEAVIEST ELEMENTS



## A Question of Shape: A New Mechanism Governing the Survival of Superheavy Nuclei

A. Rahmatinejad, T. M. Shneidman, G. G. Adamian, N. V. Antonenko, P. Jachimowicz and M. Kowal

**ECT*, Trento, 14–18 September 2026**

# The central question is dynamical, not only static

**Cold structure**

At $T = 0$, shell corrections can generate a deep spherical or deformed pocket in an otherwise very flat macroscopic landscape.

**Hot-fusion condition**

The compound nucleus is produced with $U \sim 30$–$50$ MeV. Shell and pairing correlations are then attenuated, and the equilibrium minimum may move in deformation space.

**Question addressed here**

Does a cold spherical minimum remain the relevant configuration for the one-step competition $\Gamma_n/\Gamma_f$, or does differential shell damping favor a deformed hot equilibrium?

# Hot fusion probes the regime where shell structure is changing

- Coulomb repulsion nearly cancels the macroscopic surface restoring force.
- The liquid-drop contribution is therefore flat over a broad deformation domain.
- Binding pockets and fission barriers depend strongly on microscopic shell corrections.
- At $U \sim 30$–$50$ MeV, occupations around the Fermi energy are thermally redistributed.

$$E_{\mathrm{tot}}(\beta, U) = E_{\mathrm{mac}}(\beta) + E_{\mathrm{mic}}(\beta, U)$$

$$\left| \frac{\partial E_{\mathrm{mac}}}{\partial \beta} \right| \text{ small,}$$

$\Delta E_{\mathrm{mic}}(\beta, U)$ can relocate the minimum.

**Consequence**

The rate of microscopic damping can matter as much as the cold shell correction itself.

# The macroscopic–microscopic balance defines the cold landscape

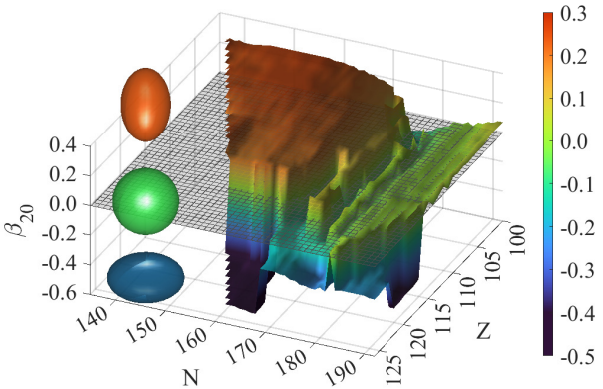
$$E_{\mathrm{bind}}(\beta) = E_{\mathrm{mac}}(\beta) + \delta E_{\mathrm{shell}}(\beta) + \delta E_{\mathrm{pair}}(\beta). \tag{1}$$

- $E_{\mathrm{mac}}$: smooth liquid-drop contribution.
- $\delta E_{\mathrm{shell}}$: oscillatory correction from bunching and gaps in the single-particle spectrum.
- $\delta E_{\mathrm{pair}}$: additional correlation energy from pairing.

**Why superheavy nuclei are special**

The cold equilibrium shape is not dictated by a strong macroscopic minimum; it is selected by relatively small, shape-dependent quantum corrections.

# Cold superheavy nuclei span several competing shapes




- spherical,
- prolate,
- oblate,
- superdeformed oblate.

**Reading the map**

Nearby isotopes can occupy qualitatively different minima; the $Z \geq 118$ region is not structurally uniform.

# Heating restores sphericity in lighter nuclei, but not necessarily in SHN

## Typical lighter nucleus

1. Macroscopic energy favors $\beta \approx 0$.
2. Shell effects may create a deformed cold minimum.
3. Heating quenches the shell contribution.
4. The macroscopic spherical minimum re-emerges.

## Superheavy nucleus

1. Macroscopic PES is flat or soft.
2. Shell effects provide the main stabilization.
3. Their damping is deformation dependent.
4. A deformed minimum can outlive a cold spherical pocket.

thermal shape evolution $\neq$ universal return to $\beta = 0$.

# Three linked claims organize the analysis

1. **Thermodynamics:** an isolated nucleus is microcanonical globally, but intrinsic degrees of freedom can be treated canonically at each frozen deformation.
2. **Microscopic mechanism:** spherical spectra contain large quasi-degenerate multiplets; thermal occupation smearing attenuates their shell free-energy correction faster.
3. **Survival implication:** damping raises the daughter potential energy and reduces the energy available in the neutron-emission numerator; deformation-dependent level density partly compensates this hindrance.

**Scope**

The final result concerns the static, one-step width ratio $\Gamma_n/\Gamma_f$; it is not yet a full multi-step evaporation-cascade survival probability.

# Strict energy conservation makes the global description microcanonical

$$E_0 = U + E_{\mathrm{pot}}^{\mathrm{GS}} = U^*(\beta) + E_{\mathrm{pot}}(U^*, \beta)\,. \tag{2}$$

- $E_0$ is fixed for the isolated compound nucleus.
- $U$ is measured relative to the ground-state potential $E_{\mathrm{pot}}^{\mathrm{GS}}$.
- $U^*(\beta)$ is the intrinsic excitation available at a specified shape.
- Changing $\beta$ redistributes energy between the potential and intrinsic sectors.

**Immediate implication**

There is no single excitation energy or temperature that can be assigned to all deformations without solving the energy constraint.

# The effective hot PES contains shape-dependent microscopic damping

$$E_{\mathrm{pot}}(U^*, \beta) = E_{\mathrm{mac}}(\beta) + E_{\mathrm{mic}}(U^*, \beta), \tag{3}$$

$$E_{\mathrm{mic}}(U^*, \beta) = \delta F_{\mathrm{shell}}(T_\beta) + \delta F_{\mathrm{pair}}(T_\beta). \tag{4}$$

- The macroscopic contribution is taken as excitation independent.
- Shell and pairing corrections are evaluated as free-energy corrections.
- Their damping is computed at the local temperature $T_\beta$ fixed by Eq. (2).

**Terminology**

$E_{\mathrm{pot}}(U^*, \beta)$ is an *effective potential-energy surface under a microcanonical constraint*, not a global isothermal free-energy surface.

# Adiabatic separation permits a local canonical calculation

**Slow variables**

Collective shape coordinates $\beta = (\beta_{20}, \beta_{22}, \ldots)$ evolve on a comparatively long timescale.

**Fast variables**

At fixed $\beta$, intrinsic quasiparticles redistribute energy rapidly and are approximated by a canonical ensemble.

$$\tau_{\text{intrinsic}} \ll \tau_{\text{collective}}$$

global microcanonical

$$\Downarrow$$

local canonical at fixed $\beta$

**Assumption**

The separation of timescales is an adiabatic approximation, not an exact identity.

# The temperature must be solved separately at every deformation

$$U(T_\beta) + E_{\mathrm{pot}}(T_\beta, \beta) = E_0, \tag{5}$$

$$U(T_\beta) = U^*(\beta). \tag{6}$$

## Self-consistent loop

For a trial $T_\beta$, compute quasiparticle occupations, entropy and microscopic corrections; update $E_{\mathrm{pot}}$ and $U$ until the fixed-$E_0$ constraint is satisfied.

$$\beta_1 \neq \beta_2 \quad \Rightarrow \quad E_{\mathrm{pot}}(\beta_1) \neq E_{\mathrm{pot}}(\beta_2) \quad \Rightarrow \quad T_{\beta_1} \neq T_{\beta_2} \text{ in general.} \tag{7}$$

## Practical meaning

Comparing two shapes at the same imposed temperature would violate the intended microcanonical construction unless their energy balances happen to coincide.

# Energy, entropy and level density connect the two descriptions

For an unpaired spectrum with occupation $n(\varepsilon)$,

$$n(\varepsilon; T, \lambda) = \frac{1}{1 + e^{(\varepsilon - \lambda)/T}}, \tag{8}$$

$$E(T) = 2 \int n(\varepsilon)\, \varepsilon\, g(\varepsilon)\, d\varepsilon, \tag{9}$$

$$S(T) = -2 \int [n \ln n + (1 - n) \ln(1 - n)]\, g(\varepsilon)\, d\varepsilon. \tag{10}$$

A saddle-point inversion gives schematically

$$\rho(E, \beta) \simeq \frac{e^{S(E,\beta)}}{(2\pi)^{3/2} \sqrt{D(E, \beta)}}. \tag{11}$$

**Physical link**

Thermal occupation smearing changes both $E_{\mathrm{mic}}$ and the phase space $\rho$ that enters decay widths.

# Finite-temperature BCS replaces particles by quasiparticles

$$E_k = \sqrt{(\varepsilon_k - \lambda)^2 + \Delta^2}, \tag{12}$$

$$f_k = \frac{1}{1 + e^{E_k/T}}, \tag{13}$$

$$n_k(T) = \frac{1}{2}\left[1 - \frac{\varepsilon_k - \lambda}{E_k}\tanh\left(\frac{E_k}{2T}\right)\right]. \tag{14}$$

- $\Delta$ opens the pairing gap around the Fermi energy.
- $f_k$ is the quasiparticle occupation; $n_k$ is the particle occupation.
- As $T$ grows, occupations become smoother and pairing weakens.

**Why it matters here**

Both shell and pairing contributions must be damped consistently before the hot PES can be compared across deformations.

# The gap and particle number are determined self-consistently

$$\frac{2}{G} = \sum_k \frac{1}{E_k} \tanh\left(\frac{E_k}{2T}\right), \tag{15}$$

$$N = 2\sum_k n_k(T), \tag{16}$$

$$S_{\mathrm{qp}} = -2\sum_k \left[f_k \ln f_k + (1-f_k)\ln(1-f_k)\right]. \tag{17}$$

One convenient energy expression is

$$E^{\mathrm{BCS}} = 2\sum_k \varepsilon_k n_k - \frac{\Delta^2}{G} - G\sum_k n_k^2, \qquad F^{\mathrm{BCS}} = E^{\mathrm{BCS}} - TS_{\mathrm{qp}}. \tag{18}$$

## Model dependence

The numerical result depends on the single-particle Hamiltonian, pairing window, smoothing prescription and treatment of odd systems.

# The shell correction is a difference of free energies

$$F(T) = E(T) - TS(T), \tag{19}$$

$$\delta F_{\mathrm{shell}}(T) = F(T) - \widetilde{F}(T) \tag{20}$$

$$= \big[E(T) - \widetilde{E}(T)\big] - T\big[S(T) - \widetilde{S}(T)\big]. \tag{21}$$

- Discrete spectrum: $g(\varepsilon) = \sum_k \delta(\varepsilon - \varepsilon_k)$.
- Smooth reference: $\widetilde{g}(\varepsilon)$ from Strutinsky averaging.
- Heating broadens occupations around $\lambda$ and reduces the oscillatory discrete-minus-smooth difference.

**Important wording**

Deformation splits spherical multiplets. Heating does not itself lift degeneracy; it smears occupations and attenuates the shell free-energy correction.

# Pairing adds a second microscopic free-energy correction

$$\delta F_{\mathrm{pair}}(T) = \left[F^{\mathrm{BCS}}(T) - F^{\mathrm{BCS}}_{\Delta=0}(T)\right] \tag{22}$$

$$- \left[\widetilde{F}^{\mathrm{BCS}}(T) - \widetilde{F}^{\mathrm{BCS}}_{\Delta=0}(T)\right], \tag{23}$$

$$E_{\mathrm{mic}}(U^*, \beta) = \delta F_{\mathrm{shell}}(T_\beta) + \delta F_{\mathrm{pair}}(T_\beta). \tag{24}$$

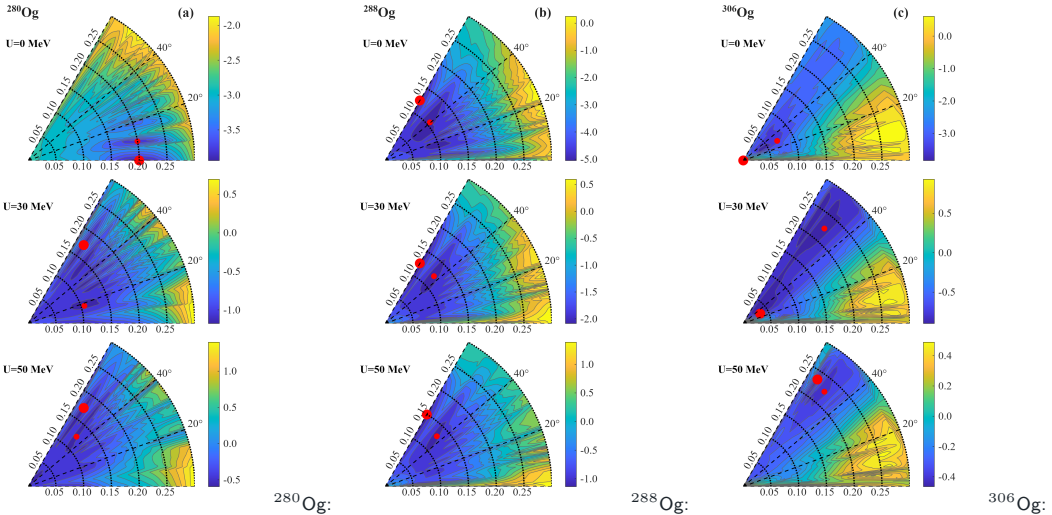
- The discrete pairing correlation is compared with its unpaired reference.
- The corresponding smooth contribution is subtracted to avoid double counting.
- Pairing normally vanishes earlier with temperature than the broad shell structure.

# The calculation closes through an energy-conserving iteration

1. Choose nucleus and deformation $\beta$; calculate $E_{\mathrm{mac}}$ and the single-particle spectrum.
2. Select a trial $T_\beta$ and solve finite-$T$ BCS for $\lambda$, $\Delta$, $E$, and $S$.
3. Apply Strutinsky smoothing and form $\delta F_{\mathrm{shell}} + \delta F_{\mathrm{pair}}$.
4. Construct $E_{\mathrm{pot}}(T_\beta, \beta)$ and test $U(T_\beta) + E_{\mathrm{pot}}(T_\beta, \beta) = E_0$.
5. Iterate $T_\beta$; repeat over the $(\beta_{20}, \beta_{22})$ mesh.
6. Locate the hot equilibrium and extract $\rho(E, \beta)$ and damping observables.

$$(\beta, E_0) \longrightarrow T_\beta \longrightarrow E_{\mathrm{mic}} \longrightarrow E_{\mathrm{pot}} \longrightarrow \beta^{\mathrm{eq}}(E_0).$$

# Three Og isotopes display three distinct thermal trajectories



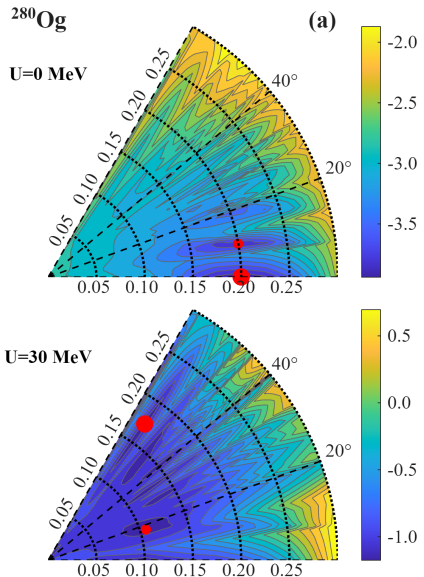

$^{280}$Og: prolate → oblate

$^{288}$Og: deformed minimum persists

$^{306}$Og: spherical → oblate/triaxial

Rows correspond to $U = 0$, $30$, and $50$ MeV; contour spacing is 1 MeV. Large red dots mark global

# $^{280}$Og undergoes a prolate-to-oblate rearrangement

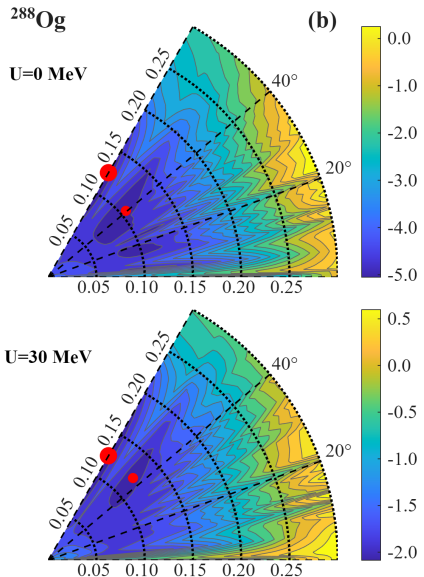



- $U = 0$: well-deformed prolate ground state.
- Around $U = 30$ MeV: the preferred basin has moved.
- At higher excitation: a well-deformed oblate configuration is selected.
- The change is not a simple reduction of $|\beta|$; the topology of the PES is reorganized.

**Interpretation**

Different shapes lose microscopic stabilization at different rates.

# $^{288}$Og keeps a deformed minimum up to 50 MeV

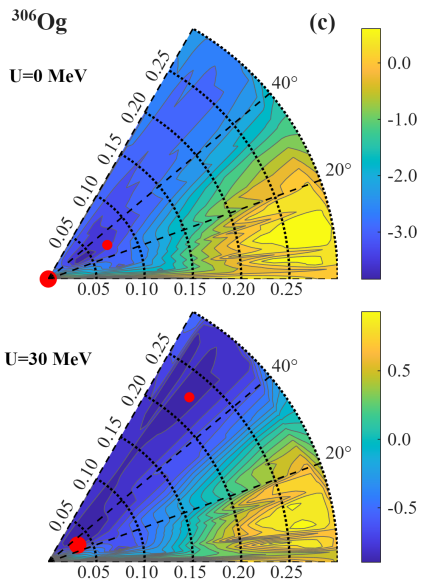



- The equilibrium lies near $(\beta_{20}, \beta_{22}) \approx (0.10, 0.10)$.
- Its location changes little between $U = 0$ and $50$ MeV.
- Here the macroscopic tendency and the more persistent deformed shell structure act in the same direction.

**Message**

Heating does not require a shape transition; it reveals which minimum remains competitive under damping.

# $^{306}$Og loses a cold spherical pocket and deforms

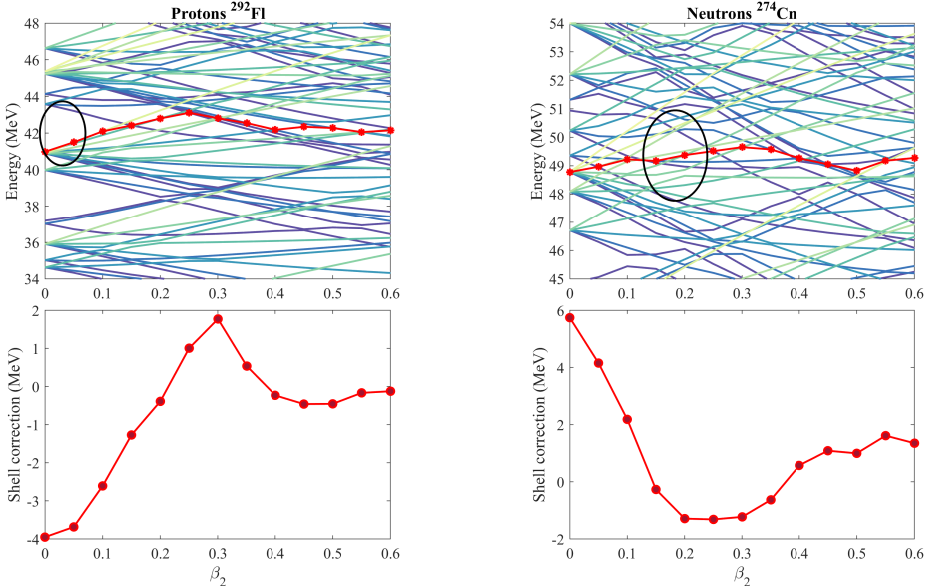



- $U = 0$: spherical minimum near the $N = 184$ shell closure.
- $U \approx 30$ MeV: rapid attenuation of spherical shell stabilization removes the cold pocket.
- The equilibrium shifts to a deformed oblate/triaxial region and remains there near $50$ MeV.

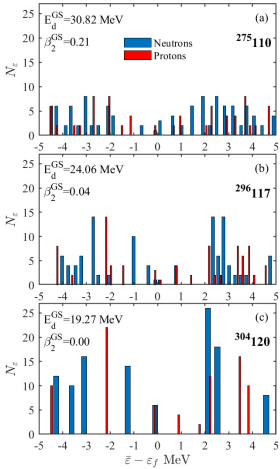
**Precise claim**

The finite-energy equilibrium can be deformed even when the cold ground state is spherical; this does not imply that all hot SHN follow the same trajectory.

# Deformation splits spherical multiplets around the Fermi surface



# Quasi-degenerate groups determine the damping rate




**How to read the bars:** their height gives the number of states in one quasi-degenerate group; their distance from the Fermi energy determines when they become thermally active; their spacing shows how gradually occupations can be redistributed.

**$^{275}$Ds: deformed, $E_d^{\mathrm{GS}} = 30.82$ MeV**

Many low bars are distributed rather uniformly. Each group contains only a few states, so successive groups become active gradually. Occupations are redistributed slowly and the microscopic correction persists to higher excitation energy.

**$^{296}$Ts: transitional, $E_d^{\mathrm{GS}} = 24.06$ MeV**

The spectrum is intermediate. Bunching is weak close to the Fermi energy, but taller groups appear at higher energies. Damping is initially moderate and then accelerates when these groups enter the thermal window.

**$^{304}$120: spherical, $E_d^{\mathrm{GS}} = 19.27$ MeV**

Only a few groups occur, but they contain many nearly degenerate states on both sides of the Fermi energy. Once the shell gap is crossed, many states become available simultaneously. Occupations are rapidly redistributed, the spherical shell correction fades quickly,

# The damping parameter is a positive energy scale

Define the local logarithmic slope where $E_{\mathrm{mic}} \neq 0$:

$$\gamma(U^*, \beta) = -\frac{d}{dU^*} \ln |E_{\mathrm{mic}}(U^*, \beta)| > 0. \tag{25}$$

Then

$$\boxed{E_d^{\mathrm{GS}} = \left[ -\frac{d}{dU^*} \ln \left| E_{\mathrm{mic}}(U^*, \beta^{\mathrm{GS}}) \right| \right]^{-1} > 0} \tag{26}$$

and the reported value is averaged over $U^* = 10$–$50$ MeV.

**Sign and meaning**

The minus sign and absolute value are essential when the stabilizing microscopic correction is negative. $E_d$ has units of MeV; it is neither a time nor a symmetry-breaking rate.

# Higher bunching near $\varepsilon_F$ correlates with faster damping

| Nucleus | $\beta_{20}^{\mathrm{GS}}$ | spectral character | $E_d^{\mathrm{GS}}$ [MeV] |
|---|---|---|---|
| $^{275}$Ds | 0.21 | sparse, well deformed | 30.82 |
| $^{296}$Ts | 0.04 | transitional | 24.06 |
| $^{304}$120 | 0 | strongly bunched, spherical | 19.27 |

- Large $E_d$: slow decay of $|E_{\mathrm{mic}}|$ with excitation.
- Small $E_d$: rapid decay of $|E_{\mathrm{mic}}|$.
- The gap to the first accessible state can delay the onset, but for comparable gaps the number of accessible states becomes decisive.

**Interpretation**

Spherical symmetry produces large multiplets; their thermal occupation smearing rapidly reduces the discrete-minus-smooth free-energy difference.

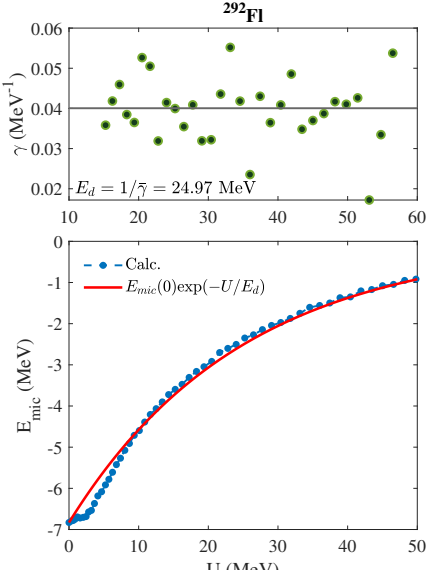
# Exponential damping turns $E_d$ into an intuitive scale

$$E_{\mathrm{mic}}(U^*, \beta^{\mathrm{GS}}) \simeq E_{\mathrm{mic}}^{\mathrm{GS}} \exp\left(-\frac{U^*}{E_d^{\mathrm{GS}}}\right), \quad (27)$$

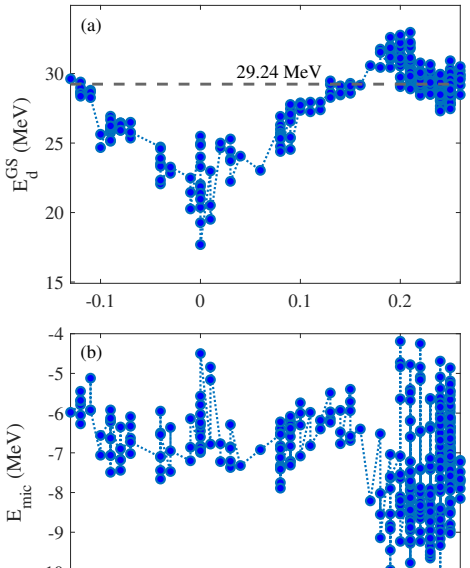
$$\gamma \simeq \frac{1}{E_d^{\mathrm{GS}}}, \quad (28)$$

$$\frac{|E_{\mathrm{mic}}(E_d)|}{|E_{\mathrm{mic}}(0)|} = e^{-1} \approx 0.368. \quad (29)$$

- $E_d \approx 19$ MeV: fast damping.
- $E_d \approx 31$ MeV: more persistent structure.



# A 353-nucleus survey reveals a deformation threshold




- Dataset: 353 nuclei with $98 \leq Z \leq 120$.
- Near $\beta_{20} = 0$: $E_d^{\mathrm{GS}}$ varies strongly, about 17–30 MeV.
- For $|\beta_{20}^{\mathrm{GS}}| \gtrsim 0.15$: $E_d^{\mathrm{GS}} \approx 30$ MeV and is comparatively stable.
- The trend follows $|\beta_{20}|$ more than the prolate/oblate sign.

**Systematic result**

Large deformation is associated with more persistent microscopic structure under excitation.

# Jahn–Teller provides a symmetry-breaking analogy

For a non-linear molecule with a partially occupied, spatially degenerate electronic ground state, a distortion can lift the degeneracy and lower the total energy:

$$\text{high symmetry} + \text{degeneracy} \longrightarrow \text{distortion} \longrightarrow \text{level splitting} \longrightarrow \Delta E < 0.$$

In a minimal linear-coupling picture,

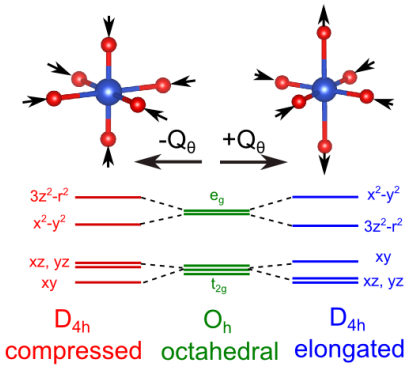
$$H(Q) = H_0 + gQ\,\hat{\tau} + \frac{1}{2}KQ^2, \qquad E_-(Q) \sim -g|Q| + \frac{1}{2}KQ^2, \tag{30}$$

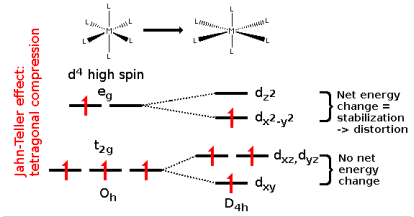
so a nonzero $Q$ can minimize the lower adiabatic branch.

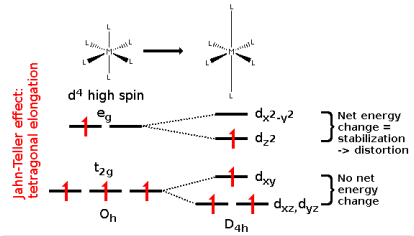
**Limit**

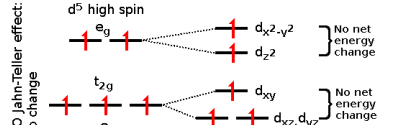
This molecular theorem is not applied literally to a finite-temperature nucleus; it supplies an organizing analogy based on degeneracy, symmetry breaking and energy competition.

# An octahedral distortion makes the molecular mechanism visible



# The shape favored when cold need not remain favored when hot

## Cold: high symmetry can maximize shell binding

- Spherical symmetry groups single-particle states into large, nearly degenerate multiplets.
- If the Fermi energy lies in a favorable shell gap, this bunching generates a large stabilizing shell correction and a deep cold pocket.

## Hot: thermal robustness can favor lower symmetry

- Excitation smears occupations, so the strongly bunched spherical spectrum rapidly loses its energy advantage.
- A deformed spectrum is already split and can damp more slowly; on a flat macroscopic landscape, an oblate or triaxial minimum may become favored.

## Jahn–Teller-like logic

Excitation exposes the instability; deformation breaks the symmetry and splits the multiplets. Cold shell binding and thermal persistence are therefore different criteria, so the landscape must be recalculated at each excitation energy.

**Limit:** Degeneracy is stabilizing only with a favorable filling and shell gap; it is not stabilizing by itself.

# The static one-step competition is a ratio of level densities

With fixed daughter ground-state and parent saddle deformations,

$$\frac{\Gamma_n}{\Gamma_f}(U^*) \propto \frac{\rho\big(A-1, \beta^{\mathrm{GS}}, E_0 - E_{\mathrm{pot}}(A-1, U^*) - B_n\big)}{\rho\big(A, \beta^{\mathrm{SP}}, E_0 - E^{\mathrm{SP}}_{\mathrm{pot}}(A)\big)}. \tag{31}$$

- $B_n$ is the neutron separation energy.
- Thermal fluctuations at the saddle are neglected in this static estimate.
- The daughter potential in the numerator must be evaluated consistently with microscopic damping.

**Scope**

$\Gamma_n/\Gamma_f$ describes one branching step. A final evaporation-residue survival probability requires the product over successive steps and all relevant channels.

# “Latent energy” is the loss of microscopic binding, not latent heat

Define the damping-induced change in the daughter microscopic correction:

$$\delta E_{\mathrm{mic}}(U^*) = E_{\mathrm{mic}}(A-1, \beta^{\mathrm{GS}}, U^*) - E^{\mathrm{GS}}_{\mathrm{mic}}(A-1). \tag{32}$$

For a stabilizing cold correction $E^{\mathrm{GS}}_{\mathrm{mic}} < 0$, damping makes it less negative, hence

$$\delta E_{\mathrm{mic}}(U^*) > 0, \qquad E_{\mathrm{pot}}(A-1, U^*) = E^{\mathrm{GS}}_{\mathrm{pot}}(A-1) + \delta E_{\mathrm{mic}}(U^*). \tag{33}$$

**Terminology**

“Latent energy” is shorthand for the energy cost of erasing microscopic stabilization. It is **not** thermodynamic latent heat: no first-order phase transition or coexistence enthalpy is assumed.

# The energy cost reduces the daughter excitation available after neutron emission

Define the numerator energy in Eq. (31):

$$E_{n,\mathrm{avail}}(U^*) = E_0 - E_{\mathrm{pot}}(A-1, U^*) - B_n \tag{34}$$

$$= E_0 - E_{\mathrm{pot}}^{\mathrm{GS}}(A-1) - B_n - \delta E_{\mathrm{mic}}(U^*) \tag{35}$$

$$= E_{n,\mathrm{avail}}^{(0)} - \delta E_{\mathrm{mic}}(U^*). \tag{36}$$

Expand the level density:

$$\ln \rho(E - \delta E) = \ln \rho(E) - \delta E \frac{\partial \ln \rho}{\partial E} + \mathcal{O}(\delta E^2), \tag{37}$$

$$\frac{1}{T} \equiv \frac{\partial \ln \rho}{\partial E}. \tag{38}$$

Therefore

$$\boxed{H(U^*) = \exp\left[-\frac{\delta E_{\mathrm{mic}}(U^*)}{T}\right]}. \tag{39}$$

# The exponential hindrance can be numerically large

For illustration, take $|E_{\mathrm{mic}}^{\mathrm{GS}}| = 6$ MeV, $E_d = 30$ MeV, and $T = 1$ MeV:

$$\delta E_{\mathrm{mic}} = 6\left(1 - e^{-U^*/30}\right), \qquad H = e^{-\delta E_{\mathrm{mic}}/T}. \tag{40}$$

| $U^*$ [MeV] | $e^{-U^*/E_d}$ | $\delta E_{\mathrm{mic}}$ [MeV] | $H$ |
|---|---|---|---|
| 30 | 0.368 | 3.79 | $2.26 \times 10^{-2}$ |
| 50 | 0.189 | 4.87 | $7.67 \times 10^{-3}$ |

**Interpretation**

These numbers illustrate the sensitivity of the numerator level density. They are not a prediction of the full residue cross section, and the linear expansion is most controlled when $\delta E_{\mathrm{mic}}$ is small on the thermodynamic scale over which $T$ varies.

# Deformation-dependent level density partly compensates the hindrance

When the hot equilibrium moves from $\beta^{\mathrm{GS}}$ to $\beta^{\mathrm{eq}}$,

$$F(E) = \frac{\rho(A-1, \beta^{\mathrm{eq}}, E)}{\rho(A-1, \beta^{\mathrm{GS}}, E)}. \tag{41}$$

With the Fermi-gas dependence

$$\rho(E, \beta) \propto \exp\left(2\sqrt{a(\beta)E}\right), \tag{42}$$

and $a(\beta^{\mathrm{eq}}) = (1+\eta)a(\beta^{\mathrm{GS}})$,

$$\ln F \approx 2\sqrt{a_{\mathrm{GS}}E}\left(\sqrt{1+\eta} - 1\right). \tag{43}$$

Thus a model-dependent $5\%$ increase in $a$ can produce $F \sim 5$–$10$ at representative SHN excitation energies. The combined static estimate is

$$\boxed{\frac{\Gamma_n}{\Gamma_f} = \left(\frac{\Gamma_n}{\Gamma_f}\right)_0 e^{-\delta E_{\mathrm{mic}}/T} F}. \tag{44}$$

# What the result changes—and what remains to be calculated

## Robust conclusions of the present analysis

- Spherical shell stabilization can damp faster than deformed stabilization.
- On a flat macroscopic PES, this can move the hot equilibrium to an oblate or triaxial shape.
- Loss of daughter microscopic binding lowers the energy available to the neutron-emission level density.
- A deformed daughter has a larger level density in the adopted estimate and therefore partially compensates the hindrance.

## Next level of validation

A quantitative synthesis prediction requires a multi-step evaporation cascade, shape fluctuations, dynamical fission, angular momentum, competing emission channels and model-uncertainty propagation.

# The cold sphere can be the most thermally fragile configuration

1. **Structure:** spherical multiplets generate strong cold shell stabilization but also strong spectral bunching near $\varepsilon_F$.
2. **Heating:** occupation smearing attenuates the spherical shell free-energy correction faster than the correction of already-split deformed spectra.
3. **Shape:** with a flat macroscopic background, the effective minimum may move from spherical to oblate/triaxial at $U \sim 30$–$50$ MeV.
4. **Decay:** the energy cost $\delta E_{\mathrm{mic}} > 0$ yields $e^{-\delta E_{\mathrm{mic}}/T}$, while deformation contributes a compensating factor $F > 1$.

**Question for discussion**

How much of this static structural correction survives in a fully dynamical, multi-step calculation of evaporation-residue formation?